Hindawi
Advances in Materials Science and Engineering
Volume 2021, Article ID 7329685, 19 pages
https://doi.org/10.1155/2021/7329685

Research Article

The Durability of High-Strength Concrete Containing Waste Tire Steel Fiber and Coal Fly Ash

Babar Ali,[1] **Erol Yilmaz**,[2] **Ahmad Raza Tahir**,[1] **Fehmi Gamaoun**,[3,4] **Mohamed Hechmi El Ouni**,[5,6] **and Syed Muhammad Murtaza Rizvi**[1]

[1]*Department of Civil Engineering (CVE), COMSATS University Islamabad (CUI)-Sahiwal Campus, Sahiwal 57000, Pakistan*
[2]*Department of Civil Engineering, Recep Tayyip Erdoğan University, Rize, Turkey*
[3]*Department of Mechanical Engineering, College of Engineering, King Khalid University, Abha 61421, Saudi Arabia*
[4]*Laboratory of Mechanics of Sousse, National Engineering School of Sousse, University of Sousse, Sousse 4054, Tunisia*
[5]*Department of Civil Engineering, College of Engineering, King Khalid University, P.O. Box 394, Abha 61411, Saudi Arabia*
[6]*Applied Mechanics and Systems Research Laboratory, Tunisia Polytechnic School, University of Carthage, La Marsa, Tunis 2078, Tunisia*

Correspondence should be addressed to Babar Ali; babar.ali@cuisahiwal.edu.pk

Received 28 July 2021; Accepted 27 October 2021; Published 12 November 2021

Academic Editor: Akbar Heidarzadeh

The demands for high-strength concrete (HSC) have been increasing rapidly in the construction industry due to the requirements of thin and durable structural elements. HSC is highly brittle. Therefore, to augment its ductility behavior, expensive fibers are used. These negative drawbacks of HSC can be controlled by incorporating waste materials into its manufacturing instead of conventional ones. Therefore, this study assessed the performance of HSC produced with different quantities of waste tire steel fiber (WSF) and fly ash (FA). WSF was used at two doses, namely, 0.5% and 1%, by volume in HSC, with low-to-medium volumes of FA, that is, 10%–35%. The studied durability parameters included rapid chloride permeability (RCP) and chloride penetration depth (CPD) by immersion method (28 and 120 days) and acid attack resistance (AAR) (28 and 120 days). Various basic mechanical properties of HSC were also analyzed, such as compressive strength (f_{CM}), modulus of elasticity (E_{CM}), splitting-tensile strength (f_{CTM}), and modulus of rupture (f_{CRM}). The results revealed that the damaging effect of WSF on the RCP resistance of HSC is probably due to the high conductivity of steel fibers. However, test results of *CPD* showed that WSF produced insignificant changes in chloride permeability of HSC. Furthermore, when made with FA, WSF-reinforced HSC yielded very low chloride permeability. Both WSF and FA contributed to the improvement in the *AAR* of HSC. WSF was highly useful to tensile properties while it showed minor effects on compressive properties (f_{CM} and E_{CM}). Optimum ductility and durability can be achieved with HSC incorporating 1% WSF and 10%–15% FA.

1. Introduction

The impacts of cement concrete manufacturing and its uses are quite complex to comprehend. Some impacts are positive, and others are negative, depending on the situation. Portland cement is the vital ingredient of concrete that has various environmental, economic, and social impacts. The impacts of cement also contribute to those of the concrete. The cement industry alone releases about 7% of the total greenhouse emissions produced all over the world [1]. Rapid growth in urban populations and the requirement of modern infrastructure have increased the demand for cement, which consequently reflects badly on the quality of the environment and social life. About 0.7–1 kilogram of global warming gases is produced due to 1-kilogram production of Portland cement, depending on the type of energy source and technology employed to manufacture cement [2]. While the other ingredients of concrete such as sand and gravels have a small CO_2 footprint, their cost and CO_2 footprint largely depend on their transportation distances between the

quarry and concrete batching plant. Therefore, about 85% of emissions of cement concrete are dependent on the binder constituent of concrete [3, 4]. The most effective way to control the environmental impact of concrete is to minimize its cement consumption. This can be achieved by the utilization of industrial waste powders that possess pozzolanicity and hydraulicity. The substitution of a small and medium volume of cement with these waste powders can drastically reduce the CO_2 footprint of concrete. However, the efficacy of potential cement substitution materials should be assessed properly in terms of their contribution towards durability and mechanical performance. The cost to strength [5, 6] or CO_2 footprint to strength ratio analysis [7] should always be performed to judge the technical performance of cementitious materials.

Fly ash (FA) is a common waste mineral powder, which is a product of pulverized fuel ash burning for electric power generation. FA incorporation into cement concrete cannot only decrease the CO_2 footprint of concrete, but it can also resolve waste disposal problems associated with high volumes of coal ashes. FA can help in gaining a circular economy in modern-day concrete manufacturing. Pakistan relies heavily on nonrenewable supplies of energy, such as coal-fed power plants. Therefore, abundant supplies of FA are available in this country. FA is rich in alumina-silica, and it has minor amounts of calcium and iron oxides. It qualifies as a potential cement replacement material [8]. The effects of FA on the properties of concrete have been studied properly. It helps in the slow consumption of residual portlandite $Ca(OH)_2$ and positively affects the resistance of concrete against water absorption, chloride attack, and drying shrinkage [9–11]. Low levels of FA can cause minor improvements in the mechanical performance of concrete [12], but its high levels drastically reduce mechanical strength [7, 13]. The degree of the effectiveness of FA depends on its fineness, chemical composition, and unburnt carbon content [14–17]. Generally, FA with high fineness and low carbon content is considered suitable for concrete applications.

Due to the increasing information gained related to material availability, design, and construction techniques, the practical scope of high-strength concrete (HSC) applications has been expanded dramatically. Rising inclination towards lightweight elements, large spans in buildings and bridges have increased the demands for HSC. However, there is a faction among designers unwilling to use HSC owing to its some drawbacks compared to conventional normal strength concrete (NSC) [18]. To begin with, HSC has a low f_{CTM} compared to its f_{CM}. The increase in the strength class of concrete reduces the ratio between f_{CTM} and f_{CM} [19]. This means that the gain in f_{CTM} achieved due to the low water-cement ratio is not proportional to the gain in f_{CM}. Due to low ductility, HSC is extremely brittle in fire temperatures. Due to a dense microstructure, the fire resistance of HSC is incredibly lower than the NSC [20].

The brittleness issue of HSC can be addressed by using fibers. Various options for fiber reinforcements are available, such as steel, carbon, polypropylene, polyvinyl, and glass fibers [21–23]. The use of fibers substantially enhances the tensile and fracture toughness of HSC. The selection of fiber type varies depending upon the application of HSC. Fiber addition is highly useful in enhancing f_{CTM} and flexural strength f_{CRM} of HSC [22]. In short, fibers can overcome the inherent issue of brittleness associated with both plain HSC and NSC. Research has shown the negative effects of fiber addition on the economy and the environmental impact of concrete [24]. High transportation distances significantly increase the cost and CO_2 footprint of fibers [24]. Their small doses can noticeably increase the cost and CO_2 footprint of concrete. Fiber addition also requires technical supervision; it creates workability issues when used in HSC. Therefore, the use of additional measures and materials to control the quality of concrete can increase the final cost. Therefore, the selection of fiber type should be made based on a comprehensive cost to benefit ratio analysis.

The development of ductile, cheap, and environment-friendly HSC is not possible without considering the less energy-intensive fibers compared to industrially manufactured fibers available at distant locations. Currently, researchers are investigating the potential of waste tire steel fibers (WSF) as the fiber reinforcement in cement concrete. Since WSF is composed of ultra-high-strength steel wires, which are designed for good fatigue resistance, it can become a potential fiber reinforcement material. WSF behaves similar to virgin steel fiber to a great extent, considering the properties of ultra-high performance concrete [25]. Considering the wider availability of old waste tires, WSF can become a local fiber-reinforcement material in all regions of the world, so high transportation costs can be avoided by adopting WSF instead of industrial fibers.

New steel fiber and WSF behave similarly as fiber reinforcement due to the same material. Small doses of WSF can be useful to f_{CM} of concrete, whereas using a large dose of WSF can lessen the f_{CM} of concrete [26]. A high dose of WSF increases the porosity of concrete due to workability issues that reflect badly in terms of compression stiffness of concrete [26]. WSF can postpone the collapse of concrete under compression; it can ensure ductile and slow cracking with a significant warning before collapse [27]. The effect of WSF on the properties of concrete significantly depends on the length, shape, texture, and residual rubber content of fiber [28]. The incorporation of 0.46% volume of irregular-shaped WSF in concrete improved its f_{CM} by 25% [29]. At the same volume of 0.75% WSF and new steel fibers, f_{CTM} of concrete increased by 28% and 26%, respectively, whereas by the use of WSF carrying mixed filament lengths, f_{CTM} of plain concrete was increased by about 50% [30, 31]. Similar to compressive behavior, the postpeak flexure response of concrete depends on the type, dose, and the number of filaments per unit volume. f_{CRM} of concrete significantly increases with the rise in WSF dosage [32, 33]. WSF provides a crack-arresting mechanism that helps in delaying the onset of rupture failure of concrete [31, 34–37].

The incorporation of FA and WSF into HSC can integrate the benefits of ductility, durability, and ecofriendliness. The simultaneous use of waste mineral admixtures and fibers proves beneficial in three different ways: (1) fine particles of mineral admixtures can improve the distribution of

filaments throughout the matrix of concrete [38], [39]; (2) mineral admixtures increase the interface between filaments and binder matrix that improves the bond performance of fibers [40, 41]; and (3) some mineral admixtures reduce the water demand of concrete due to their slow hydration and filling action, hence reducing the requirement of water-reducing agents to maintain the workability of fiber-reinforced concretes [42–45]. Due to these benefits, fibers and mineral admixture addition show some synergistic results on the performance of concrete [9]. There are very few studies that investigate the combined behavior of FA and WSF. However, many studies are available related to the combined behavior of industrial fibers and waste mineral admixtures (i.e., FA, silica fume, slag, etc.) [46–48]. The combined behavior of WSF and mineral admixture was studied by Mastali and Dalvand [27]. They found that the combined addition of silica fume and WSF improves the overall toughness and strength of concrete.

Very little information is available on the durability behavior of HSC made with the combined incorporation of WSF and FA. Moreover, information on mechanical behavior is also deficient. Due to already explained environmental, economic, and ductility benefits, the combined effect of WSF and FA should be properly investigated on the properties of HSC. Therefore, this research aimed to evaluate the effects of different combinations of FA (0, 10, 15, 25, and 35%) and WSF (0, 0.5, and 1%) on the properties of HSC. The examined durability parameters involve RCP and CPD by immersion method (at 28 and 120 days) and AAR (at 28 and 120 days). Various basic mechanical properties of HSC were also studied experimentally, such as f_{CM}, f_{CTM}, f_{CRM}, and E_{CM}. The findings of this research fill an important research gap related to the durability of waste tire steel fiber-reinforced concrete. Moreover, the combined effect of FA and WSF on both durability and mechanical properties of HSC has never been studied before.

2. Materials and Methods

2.1. Constituent Materials

2.1.1. Binding Materials. HSC mixes were prepared with 53-grade cement, which was used as the major binder. It is qualified as "Type-I cement" per ASTM C150 [49]. FA containing a low percentage of lime was acquired from a local coal power plant. It was a by-product of bituminous coal. The generation of FA was estimated to be 10% of the annual cement production of Pakistan. The composition of the FA is Class F type, known for pozzolanicity potential but low hydraulicity. Important properties of FA and 53-grade cement are given in Table 1.

2.1.2. Aggregates. Quarry sand of "Lawrencepur" was used as fine aggregate to manufacture HSC. This sand is recommended for good-quality concrete production in Punjab, Pakistan. This coarse-grained sand has a good distribution of particle sizes and has a "fineness moduli" of 2.92. Crushed dolomite sandstone was used as coarse aggregate. This aggregate was derived from Kirana Hills of Sargodha, Punjab, Pakistan. Engineering properties of fine and coarse aggregates are given in Table 2, which were important inputs in the mix design procedure of HSC. The diversity in particle sizes of both "quarry sand" and "crushed coarse aggregate" is shown in Figure 1. The maximum aggregate sizes for "fine" and "coarse" aggregates are 4.75 and 12.5 mm, respectively.

2.1.3. WSF. WSF used in this research was derived from old waste tires of truck vehicles. The tire-bead wires, when removed from waste tires, contained residual rubber. Therefore, heat treatment was applied to remove the rubber particles from steel wires. Removing rubber particles is necessary to ensure a good bond between fibers and the matrix of the concrete. Moreover, rubber reduces f_{CM} of concrete owing to its low density [28]. Finally, clean steel wires were chopped into lengths of about 30 mm. WSF consists of spun filaments as can be noticed in Figure 2. The diameter of each filament was about 1.2 mm. WSF also contains microsteel wires that were twined around the main filament in the tire bead. These small wires may provide hybrid (mixed-length and mixed-diameter effects) of fibers on the properties of HSC.

2.1.4. Water-Reducing Agent and Water. The desired workability of an HSC mixture was achieved by using a commercial third-generation water-reducing agent "ViscoCrete 3110." It also helped in controlling the drop in workability due to the addition of WSF. Tap water from the concrete laboratory was used in the preparation and curing of HSC mixes. It has a pH of 7.9 and total dissolved solid content of 170 mg/L.

2.2. Design HSC Concrete Mixes with Different Combinations of WSF and FA. In this research control or reference, HSC was designed for a cubical f_{CM} of 70 MPa. This strength class was achieved by employing a water-binder ratio of 0.30. In order to achieve good workability (a slump value of 190–210 mm), the "ViscoCrete 3110" water-reducing agent was used at 0.75% by weight of binder in reference HSC. Details about the composition of a reference mix are given in Table 3. In HSC, FA was used at five different levels, 0%, 10%, 15%, 25%, and 35%, by volumetric replacement of cement. Since FA is lighter than cement, the replacement of cement with FA should be done by volume. Then, with each incorporation level of FA, three different doses of WSF, 0%, 0.5%, and 1%, by a volumetric fraction of concrete were used. Therefore, the experimental campaign studied a total of 15 concrete mixtures. Details of all 15 mixes are given in Table 3. It is worth mentioning here that plain HSC mixtures containing FA achieved the required range of workability at 0.75% dose of water-reducing agent, while all fiber-reinforced HSC mixes required a 1% dose of water-reducing agent to achieve desirable workability. The workability was because the use of WSF increased the stiffness of fresh concrete. Therefore, the loss in workability due to the fiber addition was compensated with a high dose of plasticizer. All plain mixtures (without fibers) (serial nos. 1, 4, 7, 10, 13)

Table 1: Engineering characteristics of binders used in this study.

Binder	Chemical properties						Physical properties		
	CaO	Al_2O_3	SiO_2	Fe_2O_3	LOI	PSG	Density (kg/m^3)	SSA (m^2/kg)	Soundness (%)
FA	4.3	28.4	61.0	3.4	1.4	2.31	1128	345	—
Cement	64.2	6.7	23.9	4.3	4.7	3.12	1441	321	0.09

LOI: loss on ignition; PSG: particle specific gravity; SSA: specific surface area.

Table 2: Engineering characteristics of aggregates used in this research.

Aggregate type	Particle size (mm)		WA (%)	PSG	FM
	Max	Min			
Quarry sand (fine aggregate)	4.75	0.075	0.76	2.66	2.92
Crushed sandstone (coarse aggregate)	12.5	2.36	0.79	2.72	—

WA: water absorption at 24 hrs; PSG: particle specific gravity; FM: fineness modulus.

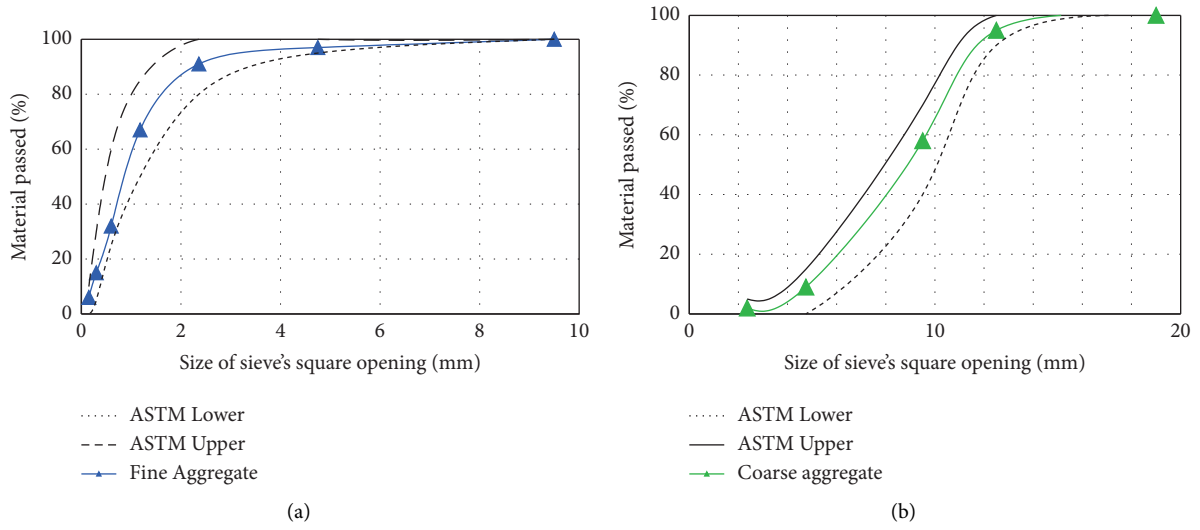

Figure 1: The aggregate size gradation curves of (a) quarry sand and (b) coarse aggregate following ASTM C33 [50].

Figure 2: An overview of a random sample of WSF.

attained a slump value of 180–210 mm, while WSF-reinforced mixes (serial nos. 2, 3, 5, 6, 8, 9, 11, 12, 14, and 15) attained slump values of 125–145 mm.

2.3. Mixing Method. HSC mixes containing WSF (serial nos. 2, 3, 5, 6, 8, 9, 11, 12, 14, and 15) were mixed in four continuous stages: (1) in the first step, cement, FA, and aggregates were mixed in machine mixer for 2 mins at a speed of 40 rev/min (revolutions per minute); (2) in the second step, half the amount of water and water-reducing agents were added to mix and blend in machine mixer continued for 2 mins at a speed of 40 revs/min; (3) in the third step, the remaining quantities of water-reducing agent and water were added and mixed, and blending was done at high speed of 60 rev/min for 2 mins; and (4) in the

Table 3: Information about the composition of concrete mixtures.

Serial. no.	Mix ID	FA (%)	WSF (%)	Cement (kg/m^3)	FA (kg/m^3)	Fine aggregate (kg/m^3)	Coarse aggregate (kg/m^3)	WSF (kg/m^3)	Water (kg/m^3)	SP (%)
1	F0WF0 (Ref)	0	0	500	0	865	904	0	150	0.75
2	F0WF0.5		0.5	500	0	859	898	39	150	1
3	F0WF1		1	500	0	852	891	78	150	1
4	F10WF0	10	0	450	37	865	904	0	150	0.75
5	F10WF0.5		0.5	450	37	859	898	39	150	1
6	F10WF1		1	450	37	852	891	78	150	1
7	F15WF0	15	0	425	56	865	904	0	150	0.75
8	F15WF0.5		0.5	425	56	859	898	39	150	1
9	F15WF1		1	425	56	852	891	78	150	1
10	F25WF0	25	0	375	93	865	904	0	150	0.75
11	F25WF0.5		0.5	375	93	859	898	39	150	1
12	F25WF1		1	375	93	852	891	78	150	1
13	F35WF0	35	0	325	130	865	904	0	150	0.75
14	F35WF0.5		0.5	325	130	859	898	39	150	1
15	F35WF1		1	325	130	852	891	78	150	1

fourth stage, measured quantities of WSF were charged into the mixer, and machine mixing was done for 4 mins at 80 revs/min to ensure proper dispersion of cement particles and fiber filaments. Plain mixes (serial nos. 1, 4, 7, 10, 13) were mixed in the first three stages which were used for the mixing of WSF-HSC mixes.

After completion of mixing, fresh concrete mixtures were tested for the slump, and mixes qualifying the workability requirements were proceeded for casting. During the casting stage, the machine mixer kept running at a low speed of 40 rev/min. Casting was completed within 4–5 mins of completion of the mixing stage.

2.4. Sample Details and Testing Methods. Six cubes of 100 mm dimensions were prepared for each mixture. The f_{CM} was determined at 28 and 120 days; three cubes of each mix were tested at one age. The standard of testing was followed as per ASTM C39 [51]. The testing setup is shown in Figure 3(a). Cylindrical samples of 100 mm diameter and 200 mm height were cast for E_{CM} testing, as shown in Figure 3(b). Three cylinders per mix were cast, of which were tested at 28 days and the remaining three 120 days. The standard of testing was adopted from ASTM C469 [52]. This test was performed to estimate the effect of WSF on the ductility of samples. For this purpose, cylindrical specimens of "100 mm diameter and 200 mm" height were prepared. Three replica samples of each mix were tested at 28 days. The standard of testing was adopted from ASTM C496 [53]. The testing overview is shown in Figure 3(c). "Flexural strength" or "modulus of rupture f_{CRM}" is a tensile property of concrete that is employed in the design equations of flexural elements, such as slabs and pavements. For each mix, three specimens having dimensions of 100 mm × 100 mm × 350 mm were tested for the calculation of f_{CRM}. f_{CRM} was determined under the third-point loading method adopted from ASTM C1609 [54]. The test setup is shown in Figure 3(d).

The chloride durability is an important characteristic of concrete that tells about the life of a reinforced structural element. *RCP* test was conducted on 100 mm diameter × 50 mm height disc specimens of each mix. The test method was adopted from ASTM C1202 [55]. *RCP* test was performed by maintaining a potential difference of 60 volts for the duration of 6 hrs. The overview of *RCP* testing is shown in Figure 4.

Chloride-ion penetration depth (*CPD*) by immersion method was also measured to understand the effects of WSF and FA on the permeability of chloride ions in the absence of applied voltage. Since WSF addition highly increases the electrical conductivity of HSC [43], it becomes more convenient to adopt the natural process of measuring chloride penetrability of HSC rather than the *RCP* test, to avoid wrong interpretation of *RCP* test results of steel fiber-reinforced concretes. For the immersion test method, six cylindrical specimens (100 mm height × 100 mm diameter) of each mix were cured in tap water for 28 days, and then air-dried for 3 days at room temperature. These air-dried specimens were then soaked in a 10% solution of sodium chloride (NaCl) salt. *CPD* was then measured by spraying 0.1 normality solution of silver nitrate ($AgNO_3$) salt, on the split surfaces of NaCl conditioned samples after periods of 28 and 120 days. Three replica samples were tested at each age to determine the average *CPD* value of each HSC mix.

Measuring the *AAR* of HSC is very important, as there are some applications where concrete experiences harsh acidic environments, such as in components of sewerage networks. Method of *AAR* testing was adopted from a previous study [9], where *AAR* was measured by quantifying the differences between fresh samples and acid exposed samples. For *AAR* testing, three replica specimens (100 mm cubes) of each mix were cured in tap water for 28 days. These specimens were then air-dried at room temperature for 3 days. Then, the samples of all mixes were exposed to sulfuric acidic (H_2SO_4) solution of 5% concentration. The change in

Figure 3: Overview of mechanical testing. (a) Compression test on 100 mm cubes. (b) Overview of axial testing for ECM determination. (c) Splitting-tensile test on "100 mm × 200 mm" cylindrical samples. (d) Overview of flexural testing on "100 mm × 100 mm × 350 mm" prismatic samples.

Figure 4: Overview of RCP testing.

the mass of specimens was measured after exposure periods of 14, 28, 56, and 120 days.

3. Results and Discussion

3.1. Compressive Properties

3.1.1. Compressive Strength (f_{CM}). f_{CM} of all fifteen mixes at the ages of 28 and 120 days is shown in Figure 5. Both FA and WSF addition showed mixed effects of f_{CM} depending on their percentage in an HSC mix. The 28 days f_{CM} of HSC was increased by 6% at 10% FA addition. This improvement in f_{CM} was credited to the effective filling effect and development of pozzolanic products [12, 15]. While f_{CM} of HSC decreased notably compared to the reference mix, with the rising level of FA. This could be blamed on a reduction in the overall lime content of the binder. Although smaller particles of FA provided a filling effect, at a high level, FA fails to develop necessary reactions responsible for strength. As FA particles reacted slowly with available portlandite,

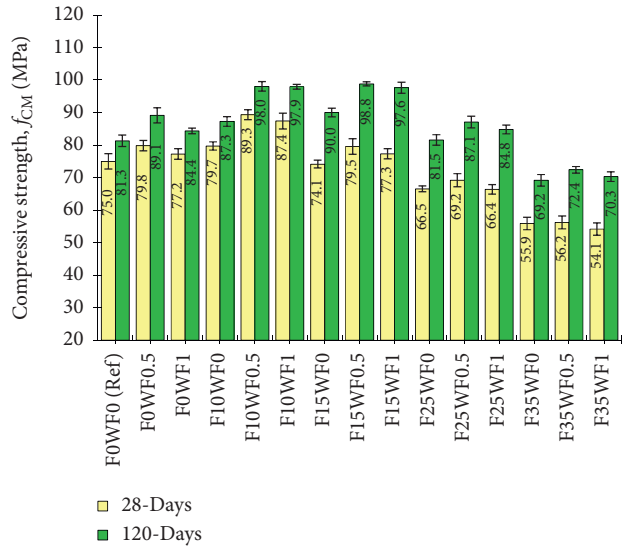

Figure 5: Effect of FA and WSF combinations on compression testing results of concrete.

HSC mixtures containing 10–15% developed noticeably (i.e., 7–11%) higher f_{CM} than the reference mix. While mix containing 25% FA showed f_{CM} similar to the reference mix at 120 days.

0.5% WSF improved f_{CM} by about 6.5% and 10% at 28 and 120 days, respectively. While 1% WSF did not show a significant effect on f_{CM} generally on all five types of plain mixes (1, 4, 7, 10, 13). At a high-volume fraction, the negative effect of WSF can be blamed on an increase in porosity and heterogeneity in the HSC matrix. A high volume of fibers produces small void pockets that decrease the efficiency of fibers contributing to the compression stiffness of concrete. Similar behavior was observed with WSF in another study [37]. Moreover, new steel fiber also showed mixed effects on f_{CM} of HSC with varying doses [56, 57]. High volume doses of fibers were not effective in increasing the peak-load capacity, but these were beneficial to the postpeak response. The high volume of WSF restricted the sharp failure and helped in sustaining a noticeable residual strength after peak load. The failure patterns of plain HSC and WSF-HSC are shown in Figure 6.

The combined effect of WSF and FA on f_{CM} of HSC at 28 and 120 days can be observed in Figure 7. Maximum f_{CM} was shown by HSC containing 0.5% WSF and 10–15% FA because both 0.5% WSF and 10–15% FA were individually helpful to f_{CM}; therefore, their combined addition significantly improved f_{CM}. Mix no. 5 (F10WF0.5) showed 19% and 21% greater f_{CM} than reference mix at 28 and 120 days, respectively. It is also worth mentioning that, due to the increase in age and hardening of the binder with 10–15% FA, 1% WSF showed a similar effect on f_{CM} compared to 0.5% WSF at 120 days. An increase in age may improve the bond of fibers with HSC's matrix. Therefore, F10WF1 showed performance similar to FA10WF0.5 at 120 days.

At 120 days, maximum f_{CM} was shown by FA15WF0.5, which was 22% higher than that of the reference mix. At 120 days, mixes incorporating 0.5–1% WSF and 10–25% FA showed noticeably higher f_{CM} than the reference mix. These results showed the usefulness of ecofriendly FA and WSF in improving f_{CM}. The combined addition of FA and WSF not only improves the mechanical and ductility performance of HSC but also can substantially decrease cost and carbon footprint due to a reduction in cement quantity.

3.1.2. Modulus of Elasticity (ECM). E_{CM} is a measure of compression stiffness of concrete significantly within the elastic limit state of the material. The results of all HSC mixtures with different combinations of FA and WSF are shown in Figure 8. The relationship between WSF, FA, and relative E_{CM} of HSC is shown in Figure 9.

The addition of 10% FA showed a small improvement in E_{CM} of HSC. In contrast, the 28-day E_{CM} of HSC decreased considerably with the rising FA percentage. While, at 120 days, E_{CM} of HSC containing 10–15% FA was comparable with that of the reference HSC. Small percentages of FA can increase the compression stiffness by decreasing the pore size. The filling effect of small FA particles can cause a small increase in the density of concrete that improves the compressive stiffness, while pozzolanic activity also contributes to strength at lower levels of FA [7, 58]. In contrast, high-volume FA addition decreases the pozzolanic activity and inactive filler content of concrete increases. This slows the strength development and reduces E_{CM} [59].

Literature has shown insignificant effects of new steel fibers on E_{CM} [60] because fibers do not activate when the loading is well within the elastic limit of concrete. Therefore, E_{CM} of HSC entirely depends on the development level of basic ingredients of concrete. The addition of 1% WSF proved detrimental to E_{CM} as it caused a small reduction of 2–5% in E_{CM} because, at a high-volume fraction, the density of concrete might decrease due to the poor dispersion of fibers. 1% new steel fiber addition also showed a negative effect on E_{CM} [60]. Very few studies investigated the axial stress-strain characteristics of WSF-HSC mixes. A study showed a small increase (1–8%) in E_{CM} of ultra-high

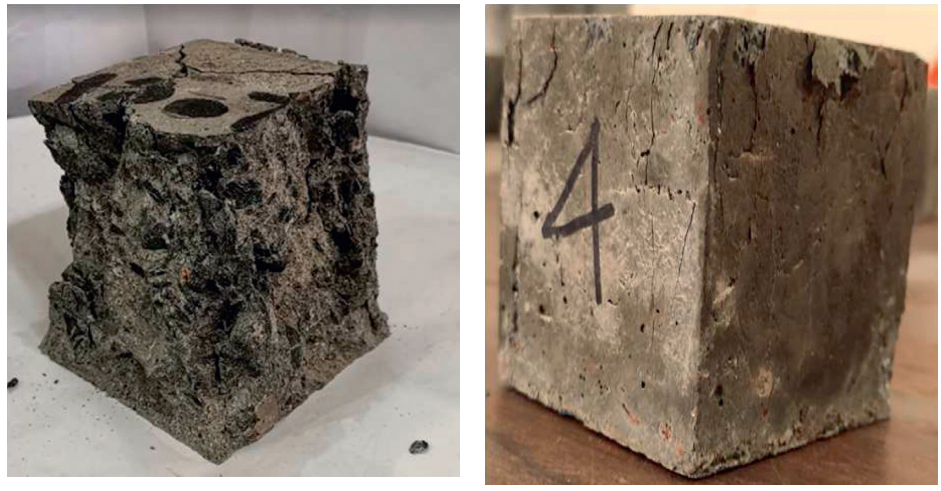

(a) (b)

Figure 6: Compression failure. (a) Cube with 0% WSF. (b) Cube with 1% WSF.

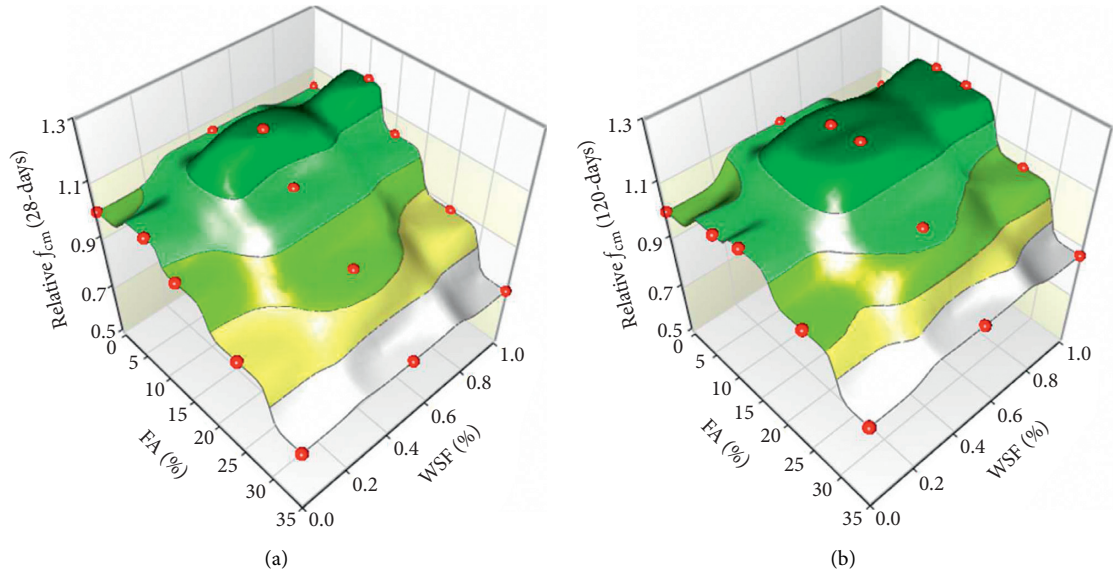

(a) (b)

Figure 7: Relationship between FA, WSF, and relative f_{CM} values of HSC: (a) 28 days and (b) 120 days.

performance concrete due to 2–3% volume of WSF [61]. In contrast, a lot of efforts are still required towards understanding the effects of WSF on E_{CM} of concrete as the deficiency on this topic has been highlighted in a recent review study [62]. However, from this study, it can be concluded that 0.5% WSF proved to be useful to E_{CM}, while 1% WSF slightly lowered the E_{CM}.

The maximum E_{CM}, 4–5% higher than reference HSC, was shown by HSC containing 10% FA and 0.5% WSF at both 28 and 120 days. The negative effect of 1% WSF was more pronounced in HSCs containing a high volume of FA because increasing FA content in the binder decreased the matrix strength and eventually the bond performance of WSF. The low strength of the matrix weakened the grip over fibers; hence, it decreased the efficiency of WSF. In contrast, the negative effect of 1% WSF on E_{CM} was more pronounced at 28 days in the HSC mix with a high volume of FA compared to the E_{CM} of these mixtures at 120 days. As the age of HSC increased, the negative effect of 1% WSF on E_{CM} reduced because the hardening of binder paste improves the bond performance of fibers [41].

3.2. Tensile Properties

3.2.1. Splitting-Tensile Strength (f_{CTM}). f_{CTM} was found out by conducting a split-tensile test on standard cylindrical samples of all mixes. The average f_{CTM} of each HSC mix with standard deviation value is shown in Figure 10. Brittleness is a major issue with the application of HSC because it has a small f_{CTM} value compared to the respective f_{CM}. Therefore, the fiber addition becomes a viable option to increase the ductility and fire resistance of HSC. As can be seen from the

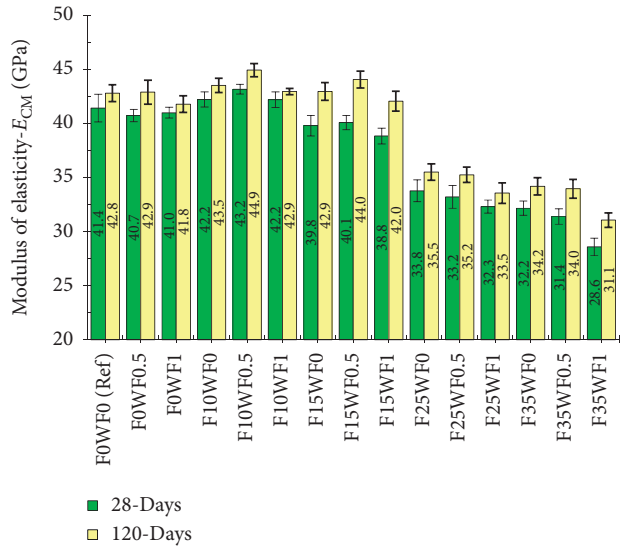

Figure 8: Effect of different combinations of WSF and FA on the $(E)_{CM}$ of HSC.

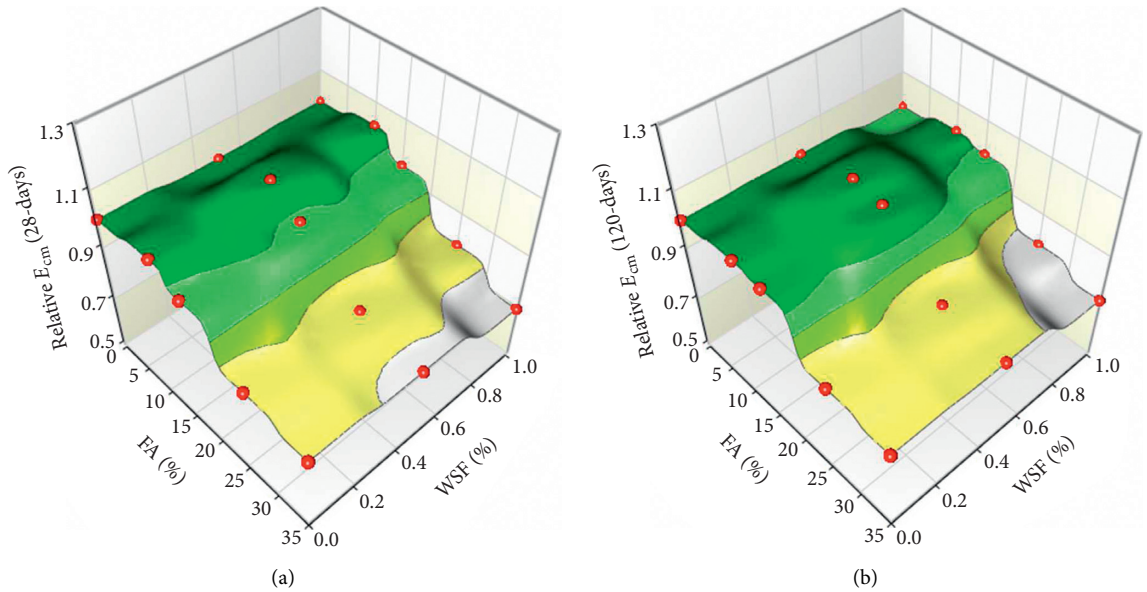

Figure 9: Relationship between FA, WSF, and relative $(E)_{CM}$ values of HSC: (a) 28 days and (b) 120 days.

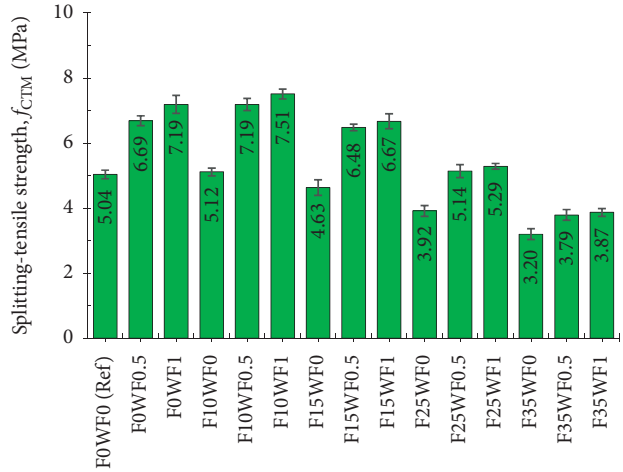

Figure 10: The f_{CTM} value of HSC with different incorporation levels of FA and WSF.

results, WSF proved very useful in advancing the tensile strength of HSC. An overall improvement of 32% and 42% was noticed in f_{CTM} of HSC (containing 0% FA) at 0.5% and 1% WSF addition. Studies have shown positive effects of WSF on f_{CTM} [63]. This improvement, as observed with industrial fibers, is credited to the crack-arresting behavior of WSF [27]. FA addition showed a negative effect on f_{CTM} of HSC. FA higher than 10% caused a drastic decline in tensile strength, whereas 10% replacement of cement with FA caused a small 2% increase in f_{CTM}. In contrast, 15, 25, and 35% FA addition reduce f_{CTM} of HSC by 8, 22, and 36%, respectively, because the decrease in strength development with the rising FA percentage in a binder and the filler effect of FA particles does not contribute to tensile strength.

The combined addition of 1% WSF and 10% FA showed an increase of 49% in f_{CTM} of HSC compared to the reference HSC mix. This showed using a smaller percentage of FA as cement replacement can synergize the benefits of using FA and WSF together. There was a certain improvement in the bond strength of WSF with the addition of 10% FA in the binder matrix. This has been observed with the combined use of FA (at a small level) and industrial steel [9] and glass fibers [58]. FA particles being spherical and smaller than cement particles can improve the particle packing in the binder matrix of HSC, in addition to the pozzolanicity potential of FA. These positive effects of a small percentage of FA reflect the improvement of the bond performance of fibers.

WSF has shown some positive effects on high-volume FA-HSC mixes. As we know, FA is ecofriendly and the cost and carbon footprint of concrete significantly drops when it replaces cement in the binder [7], but it badly affects the tensile performance of HSC. Therefore, WSF can help in controlling the drop of f_{CTM} due to the addition of a high volume of FA. The more important observation here is that HSC made with 25% FA and 1% WSF showed higher f_{CTM} than the reference HSC mix. The mix made with both FA and WSF was not just better in f_{CTM} than the reference mix, but it was also ecofriendly and cheap compared to the reference mix. WSF addition was not just useful in increasing the load at which HSC failed under splitting action. It was also very beneficial in containing the crack-width after the peak load, as shown in Figure 11. After the peak load, WSF-reinforced HSC possessed high residual strength than the plain HSC mix.

The net effect of WSF addition on f_{CTM} of HSC was reduced with the rising FA level in the binder. As FA decreased the strength of HSC, the grip of the binder over WSF weakens. Therefore, the net increase in f_{CTM} due to WSF addition was significantly influenced by the binder composition.

The ratio between f_{CTM} and f_{CM} of each HSC mix is shown in Figure 12. This ratio can be used to assess the ductility of a particular concrete mix. A higher value of the f_{CTM}/f_{CM} ratio indicates high ductility, while a lower value shows low ductility. It can be observed that the use of fibers increased the f_{CTM}/f_{CM} of HSC. The increase in f_{CTM}/f_{CM} of HSC was proportional to the reinforcement index. Figure 12 also showed that f_{CTM} of HSC increased from 6.7% to 9.3% of f_{CM} as WSF content increased from 0 to 1%. f_{CTM}/f_{CM} of FA mixes went on decreasing with the rise in FA content. This showed that the brittleness of concrete increased when a high volume of FA was used. The relationship surface between FA and WSF contents and relative or normalized f_{CTM} is shown in Figure 13. According to this surface, maximum relative f_{CTM} of HSC was achieved within 0–15% FA and 0.5–1% WSF contents. On the contrary, the lowest relative f_{CTM} was shown by mixes incorporating 35% FA for a given content of WSF.

3.2.2. Modulus of Rupture (f_{CRM}). f_{CRM} is another indirect measure of the tensile capacity of cement-based composites. The effect of different combinations of FA and WSF on f_{CRM} of HSC is shown in Figure 14. The variation in f_{CRM} results with the changing FA and WSF contents was similar to that observed in the case of f_{CTM} results. However, f_{CRM} was highly sensitive to WSF addition compared to f_{CTM}. Comparing the results of f_{CM}, E_{CM}, f_{CTM}, and f_{CRM} revealed that WSF addition yielded maximum benefits to f_{CRM}. Similar to WSF, other industrial fibers (steel, coconut, glass, polypropylene, etc.) [43, 56, 58, 64] have also shown maximum utilization in flexural behavior.

f_{CRM} of HSC increased by 56% and 78% due to the addition of 0.5% and 1% WSF, respectively. This showed a significant increment in the flexural toughness and ductility of HSC with WSF addition. On the contrary, a significant reduction in f_{CRM} was noticed at 15–35% FA addition. f_{CRM} of HSC dropped by 37% at 35% replacement of cement with FA. At high volume incorporation, FA is generally known to aggravate the mechanical properties of HSC similarly [5, 13, 65]. The common effect of FA addition was observed on the reduction level of all tested mechanical strength properties, that is, f_{CM}, E_{CM}, f_{CTM}, and f_{CRM}. It is because the change in microstructural growth is similarly reflected in compression and tensile properties.

The combination of 10% FA and 0.5–1% WSF showed superior results among all mixes. F10WF1 and F10WF0.5 showed 83% and 65% higher rupture strength than the reference mix. The synergistic effect of FA and WSF was noticed in F10WF1 and F10WF0.5. For example, the net increase in f_{CRM} due to 1% WSF addition in 0% FA-HSC was 70%, while 1% WSF showed an improvement of about 80% in 10% FA-HSC. The high net effect of WSF was achieved because of the synergistic behavior of 10% FA and 1% WSF. Improvement in the particle size distribution within HSC's matrix increases the pullout strength of WSF. However, the efficiency of WSF decreased significantly in HSC mixes containing a high volume of FA because the binder matrix containing high FA volume showed slow development and incomplete growth of microstructure at an early age.

It is generally known that FA incorporation shows some detrimental effects on the tensile properties of concrete. However, it is an ecofriendly and durable substitution of cement. The results of this study show that mixes with up to 25% FA can show better f_{CRM} than reference mix if 0.5–1% WSF is used as the reinforcement. Although choosing industrial fibers, to overcome the f_{CRM} strength loss of HSC

(a) (b) (c)

Figure 11: Splitting-tensile failure modes of HSC with (a) 0% WSF, (b) 0.5% WSF, and (c) 1% WSF.

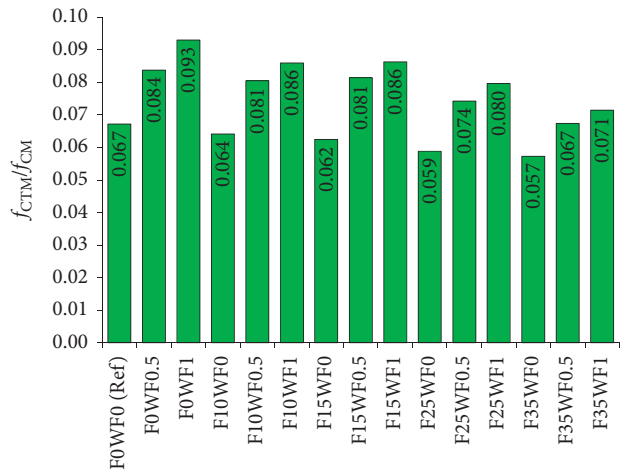

Figure 12: The ratio between f_{CTM} and f_{CM} of all HSC mixes.

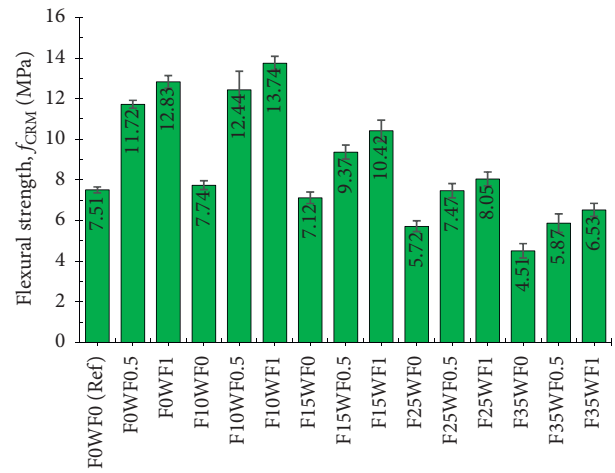

Figure 14: The f_{CRM} of each HSC mix with different incorporation levels of FA and WSF.

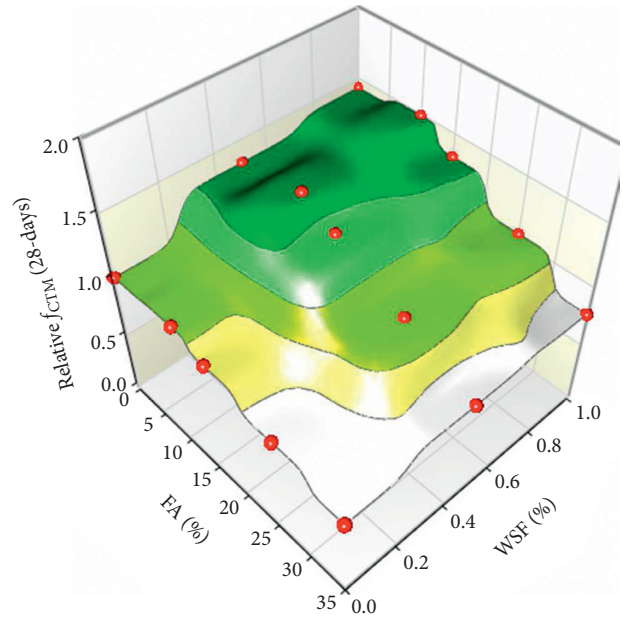

Figure 13: Relationship between WSF and FA contents and relative f_{CTM}.

due to FA, is an expensive and non-ecofriendly option, WSF, which is a waste product with minimum energy involved in its processing, can be used with FA to produce ductile and ecofriendly HSC. In addition to economic benefits, the HSC composite built with FA and WSF offers high flexural toughness and residual strength than reference HSC.

The f_{CRM}/f_{CM} ratio of each HSC mix is shown in Figure 15. It is noticed that plain HSC mixes made with or without FA showed f_{CRM}/f_{CM} ratio between 0.06 and 0.1. It means for HSC, f_{CRM} is about 6–10% of the corresponding f_{CM}. Fiber-reinforced HSC mixes yielded f_{CRM} about 16–18% of the f_{CM} value. High f_{CRM}/f_{CM} was shown by HSCs made with 0.5–1% WSF and 0–10% FA. The use of high-volume FA decreased the f_{CRM}/f_{CM} value significantly even for WSF-reinforced mixes. F35WF0, F35F0.5, and F35F1 showed f_{CRM}/f_{CM} values notably lower than the plain-reference mix (F0WF0). These findings suggested that the strength and development of the binder matrix substantially influence the efficiency of WSF. A 3-dimensional plot between relative f_{CRM}, WSF, and FA percentage is shown in Figure 16. The highest plateau (the maximum values of relative f_{CRM}) on this surface belongs to 0.5–1% WSF contents and 10% FA,

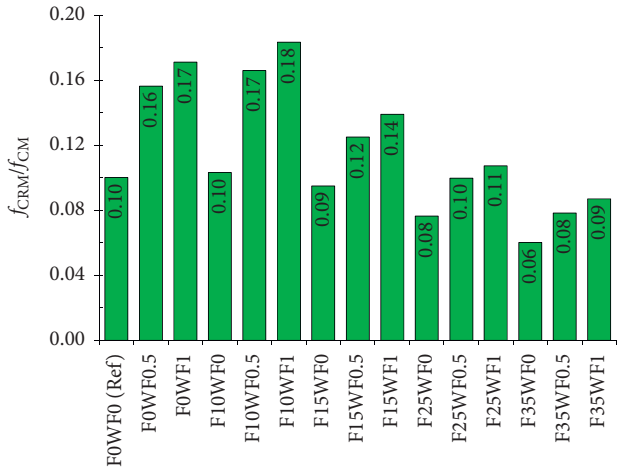

Figure 15: The ratio between f_{CRM} and f_{CM} of all HSC mixes.

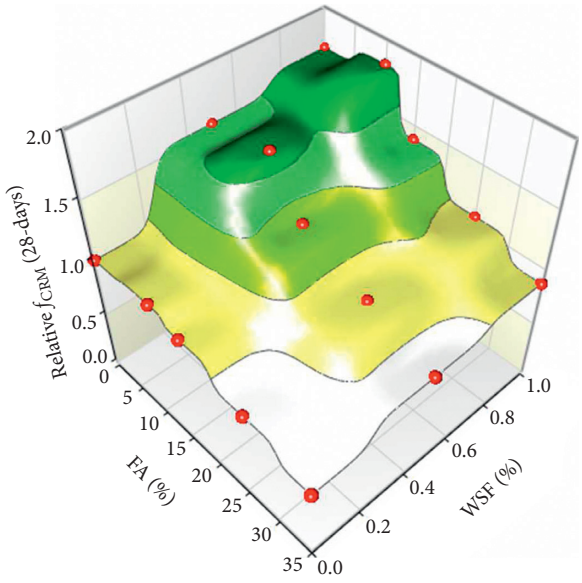

Figure 16: Relationship between WSF and FA contents and relative f_{CRM}.

while the lowest valley on the surface (the minimum values of relative f_{CRM}) is related to HSC mixes with 25–35% FA and 0–0.5% WSF contents.

3.3. Chloride Permeability Test Results

3.3.1. Rapid Chloride Permeability (RCP). *RCP* test is used for rapid assessment of chloride-ion permeability resistance of cementitious concretes. The representative *RCP* value of a mix largely depends on the microstructural density and development. Moreover, it is also affected by the ability of concrete to conduct electrical charges. The effect of WSF and FA was determined on *RCP* resistance of HSC at 28 and 120 days. The results are presented in Figure 17.

The *RCP* values of all HSC mixes are lower than 2000 coulombs, which means *RCP* of all mixes comes under the category of "low" chloride-ion permeability, according to

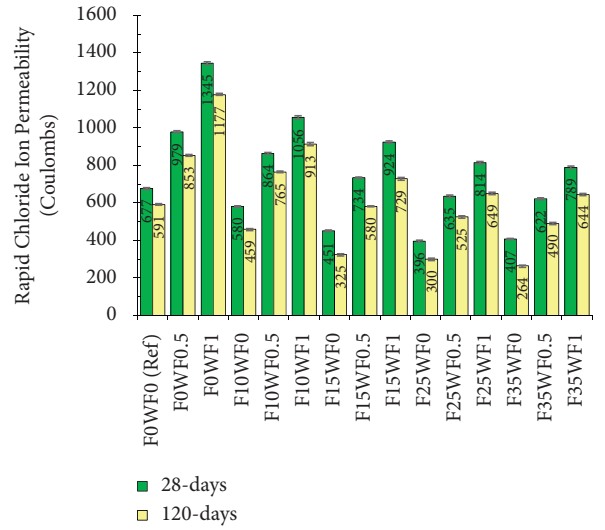

Figure 17: *RCP* of each HSC mix with different incorporation levels of FA and WSF.

Table 4. Moreover, plain mixes made with and without FA showed *RCP* values significantly lower than those noticed for WSF-reinforced mixes. *RCP* values of plain HSC mixes are lower than 1000, which indicates that plain mixes have "very low" chloride-ion permeability.

Very low *RCP* values of plain mixes are mainly because of a small water-binder ratio (i.e., 0.3). *RCP* of concrete further decreased with the rise in FA content; see Figure 18. The use of 10, 15, 25, and 35 FA decreased the *RCP* by 15%, 34%, 42%, and 40%, respectively. The decrease in *RCP* with FA inclusion in the binder is mainly credited to the filling effect of FA particles. Moreover, an increase in the tricalcium aluminate content of concrete increases the chloride binding capacity of concrete [10]. The inverse relationship between FA and *RCP* has also been observed in past research [67]. A decrease in the electrical conductivity of concrete has also been reported with the addition of slag in the binder of HSC [43].

The high electrical conductivity of WSF increased the *RCP* of HSC. About 50% and 100% increase of *RCP* was observed at the addition of 0.5 and 1% volume fraction of WSF in HSC. This immense increase in RCP indicates that WSF-HSC is more vulnerable to corrosion attacks. Not only are the main steel bars vulnerable to corrosion attack but also the filaments of WSF can degrade over time in HSC. Degradation of both WSF and main reinforcement will eventually lead to a decrease in the capacity of structural elements. The small increase in the permeability of HSC due to fiber addition may also contribute to an increase in *RCP* since permeability also favors the rapid penetration of chloride ions. A significant increase in the electrical conductivity of HSC has been observed due to the incorporation of industrial steel fiber [57]. The directly-proportional relationship between *RCP* and WSF contents is shown in Figure 19.

The use of FA significantly decreased the *RCP* of WSF-reinforced HSC. This means that FA can be used to compensate for the loss in chloride durability of HSC due to WSF

Table 4: Electrical indication of chloride durability [66].

Electrical charge (coulombs)	Chloride penetrability of concrete
>4000	Very high
2000–4000	Normal
1000–2000	Low
100–1000	Very low
<100	Insignificant

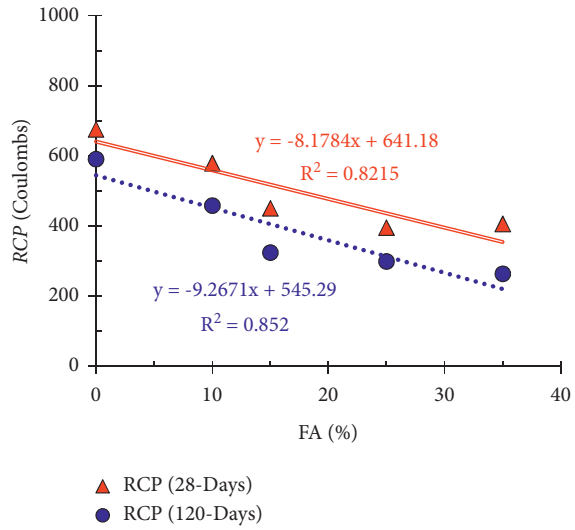

Figure 18: Relationship between FA content in binder and corresponding *RCP* values of HSC.

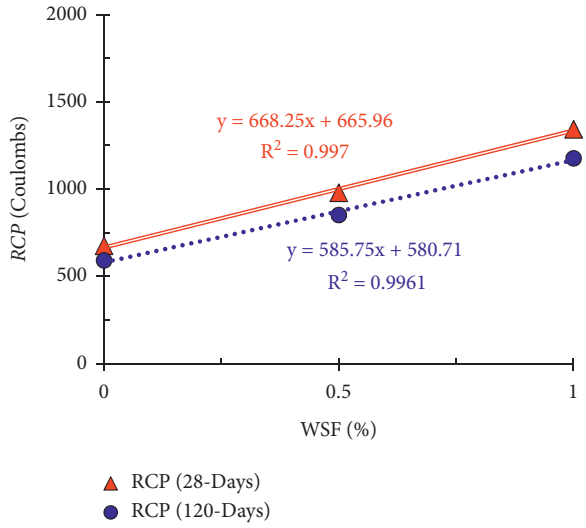

Figure 19: Relationship between WSF content and corresponding *RCP* values of HSC.

addition. To obtain *RCP* values of WSF-reinforced HSC in the range of the "very low" category, the use of 10–15% FA is necessary. The use of the high volume of FA showed high *RCP* resistance, but it reduced the strength, which would probably be the main drawback considering the application of high-volume FA in HSC. However, it is not possible to achieve an *RCP* value similar to the reference mix when using 1% WSF without considering the use of the high volume of FA.

3.3.2. Chloride Penetration Depth (CPD). The *CPD* is a reliable and more realistic measurement of chloride penetrability of cementitious material than *RCP*, which is not affected by the electrical conductivity of the material. It largely depends on the porosity, saturation of pore-solution, and microstructural growth of concrete. The *CPD* of each HSC mix after immersion in chloride solution for 28 and 120 days is shown in Figure 20.

The incorporation of FA leads to a drop in *CPD*, indicating that chloride durability of concrete increases with FA addition. As already explained in Section 3.3.1, FA improves the distribution of particle sizes in the matrix of HSC. The decrease in pore size slows the movement of the chloride-bearing medium into the concrete. Moreover, alumina silicate particles of FA have chloride binding capacity. The minimum *CPD* was shown by HSC containing 25% FA. The relationship between FA (%) and *CPD* of HSC is shown in Figure 21. The *CPD* value of HSC kept decreasing until 25% FA, while a small increase in *CPD* was observed at 35% FA. This can be explained by a decline in the microstructural growth of the binder matrix at a high volume of FA addition. However, still, all FA mixes showed notably lower *CPD* values than the reference mix.

Contrary to *RCP* test results, *CPD* test results show a small effect of WSF on the chloride permeability of concrete; see Figure 22 because the high conductivity of WSF-reinforced concrete does not affect the penetration of chloride ions in natural conditions. *CPD* was increased only by 2–7% at 0.5–1% addition of WSF. The small increase in porosity due to WSF addition is responsible for a slight rise in the *CPD*. A study has shown that chloride diffusion of concrete is not significantly affected by the electrical conductivity of the material [68]. Therefore, steel fiber addition did not increase the chloride diffusion in the concrete. HSC mixes made with the combined FA and WSF addition show *CPD* values significantly lower than the reference mix. A small increase in *CPD* caused by WSF is substantially suppressed by FA addition.

3.3.3. Relationship between CPD and RCP. The relationship between *CPD* and *RCP* values of all HSC mixes is shown in Figure 23. Since *RCP* is significantly influenced by electrical conductivity, it does not find a strong correlation with *CPD*, as *CPD* is not affected by the conductivity of the material. For plain mixes (made with or without FA), it is possible to find a strong correlation between *CPD* and *RCP* values, but for WSF-reinforced mixes, it is difficult to correlate these two parameters without considering the effect of fiber.

Figure 24 shows the relationship between *CPD*, *RCP*, and WSF content of HSC at each level of FA. The relationship is derived in the format of equation (1), where *CPD* is calculated as a function of *RCP* and volume of WSF (V_{WSF}). A and B are constants of the linear equation. *RCP* is taken as an independent variable because it is determined quickly compared to *CPD*. Therefore, *CPD* can be estimated from

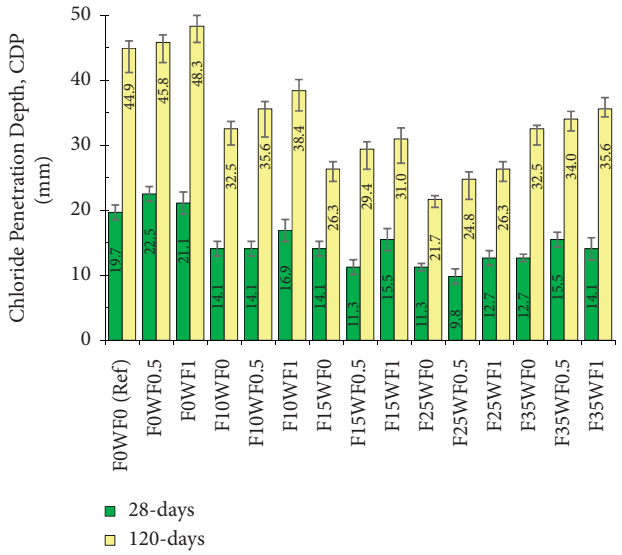

Figure 20: *CPD* of each HSC mix with different incorporation levels of FA and WSF.

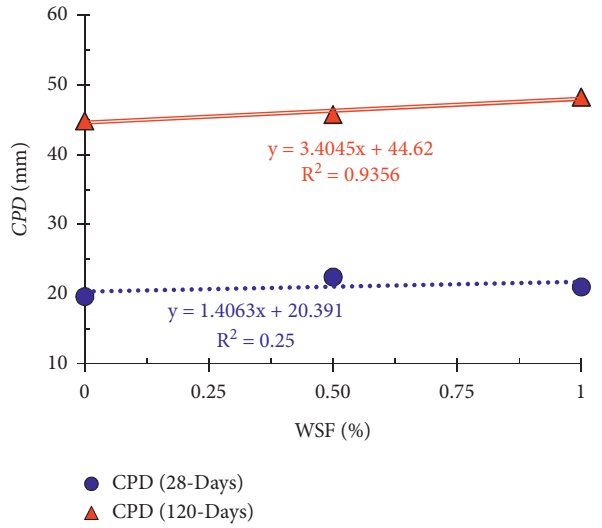

Figure 22: Relationship between WSF content and corresponding *CPD* values of HSC.

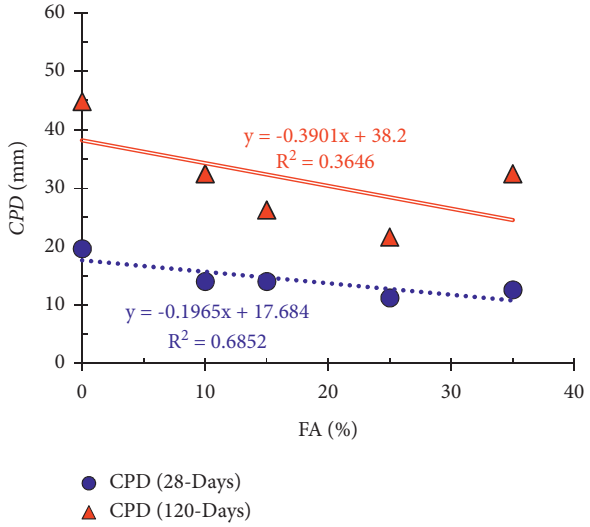

Figure 21: Relationship between FA content in the binder and corresponding *CPD* values of HSC.

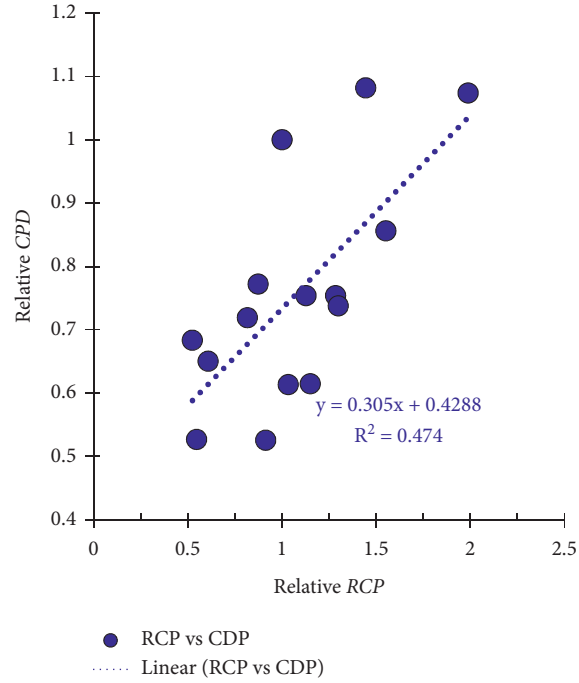

Figure 23: Relationship between *CPD* and *RCP*.

RCP for WSF-reinforced concretes. As shown in Figure 24, *CPD* and *RCP* can be correlated strongly if V_{WSF} is considered. These relationships have important implications for applications of steel fiber-reinforced concretes, as *CPD* values, which are found after a long time, can be accurately estimated from *RCP* as a function of V_{WSF}:

$$CPD = RCP \times (A \times V_{WSF} + B). \quad (1)$$

3.4. Sulfuric Acid Attack Resistance (AAR). Cementitious concretes often experience acidic environments in their application. In most cases, acidic solution dissolves both hydrated and unhydrated cementitious compounds, leading to the deterioration of the mechanical performance of concrete. If calcareous aggregates are used, they are also dissolved by acidic action. Therefore, the measurement of *AAR* becomes a related durability parameter. In this study, the durability of HSC mixes was measured in an artificial acidic medium created by a 5% solution of sulfuric acid in tap water. The results of all HSC mixtures are shown in Figure 25.

The plain HSC or reference mix showed the maximum loss in mass compared to all other HSC mixtures at both ages of testing. The *AAR* of HSC substantially increased due to the addition of both FA and WSF. As FA content increased in

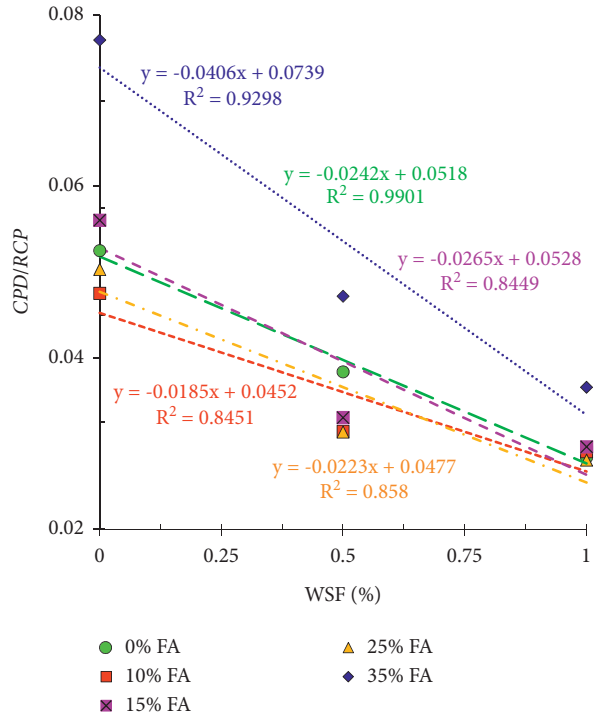

Figure 24: Relationship between CPD, RCP, and WSF content of WSF for each level of FA.

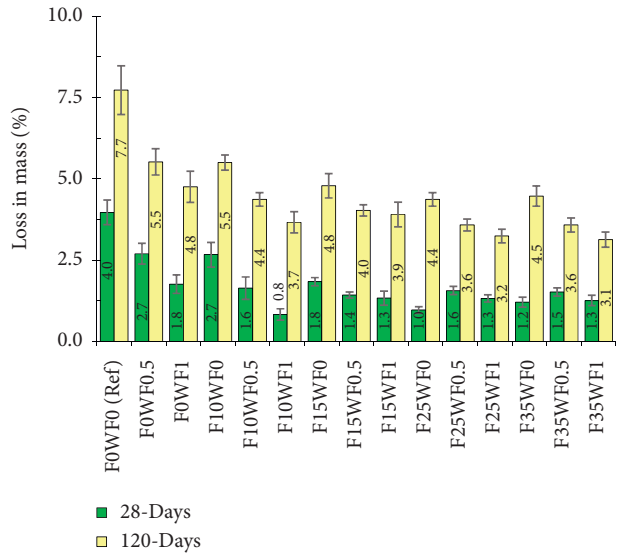

Figure 25: Loss in mass of each HSC mix with different incorporation levels of FA and WSF as a result of acid attack.

the concrete, the total alumina-silica content of the binder increased. The rise in FA causes a reduction in the calcium oxide content of the binder. The reduction in calcium hydrates and unhydrates makes the HSC resistant to acid attack. Similar observations were observed due to the addition of rice husk ash into the binder [68]. The increase in silica content and decline in lime content is the major reason responsible for the high durability of HSC in the acid attack. Another reason is that the low permeability of FA mixtures slows the movement of acidic solution into the matrix of the concrete.

The relationship between FA, WSF contents, and relative loss in mass (*LIM*) under acid attack are shown in Figure 26. This relationship shows that high *AAR* or low *LIM* under acid attack is achieved with high-level incorporation of WSF and FA. WSF increases *AAR* by its capability to hold crack propagation. Sulfate attack is accompanied by the formation of expansive salts and water. It exerts the pressure inside the binder matrix to disintegrate the microstructure of concrete and finally deteriorate the mechanical strength of HSC. WSF controls such disintegration and degradation of mechanical strength; as a result, low *LIM* was observed in mixes with fibers.

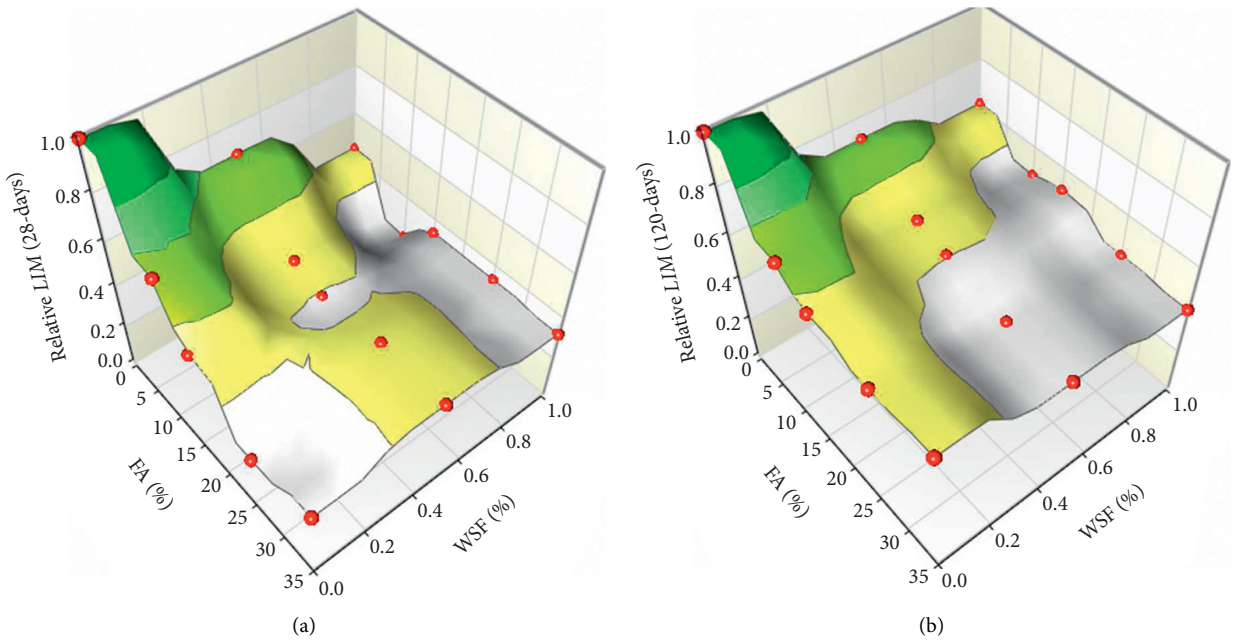

Figure 26: Relationship between FA, WSF, and relative loss in mass-*LIM* values of HSC: (a) 28 days and (b) 120 days.

Improvement in the AAR of concretes with industrial steel and glass fibers has been reported in previous studies due to their crack-bridging effects [9, 58, 69]. Mixes made with 10–35% FA and 0.5–1% WSF showed almost half disintegration under acid attack compared to the reference mixture. WSF also improved the residual strength of HSC exposed to an acidic solution.

4. Conclusions

In the present study, the combined effect of fly ash (FA) and waste tire steel fiber (WSF) was investigated on the durability and mechanical performance of high-strength concrete (HSC). The main theme of this research is the advancement in knowledge about ecofriendly and ductile cementitious composites. The following are the key findings of the present research:

(1) HSC made with low-to-medium levels of FA (10–15%) and WSF (0.5%) showed optimum f_{CM}. High-level incorporation of FA lessened the efficacy of WSF on f_{CM}. For all incorporation levels of FA, the optimum dosage of WSF is 1%. E_{CM} of HSC did not change considerably due to WSF. Lessening in E_{CM} was observed with the rising FA and WSF contents in HSC. HSC made with 0.5% WSF and 10% FA showed higher E_{CM} than the reference mix.

(2) f_{CTM} of HSC was considerably sensitive to WSF addition. The HSC made with 10% FA and 1% WSF showed maximum f_{CTM}, about 50% higher than the reference HSC mix. The splitting-tensile efficiency of WSF decreased with the rising FA percentage in the binder. Similar to f_{CTM}, f_{CRM} was also sensitive to WSF addition. Maximum f_{CRM} was shown by HSC incorporating 10% FA and 1% WSF, which was 83% higher than the reference mix.

(3) The *RCP* of HSC was increased drastically with WSF addition. 1% WSF addition caused about a 100% increase in the *RCP* of HSC mainly because of the high electrical conductivity. FA caused a decrease in *RCP* with each rising level. FA minimized the negative effect of WSF on *RCP*. However, *RCP* should not be taken as a good measure of chloride permeability capacity of steel fiber-reinforced concretes. On the contrary, *CPD* test results gave realistic values of chloride permeability capability of WSF-reinforced concretes.

(4) The *CPD* results are not affected by the electrical conductivity. Therefore, WSF addition did not show a drastic increase in *CPD*. All WSF-reinforced mixes incorporating FA showed lower *CPD* than the reference HSC mix. HSC made with 25% FA and 0.5% WSF showed 50% lower *CPD* than the reference mix. A strong mathematical correlation between *CPD* and *RCP* can be derived if the volume of WSF is considered.

(5) Both FA and WSF were extremely useful in *AAR*. Increased integrity of concrete due to the fibers and decline in calcium content of the binder is accountable for excellent acid attack durability of HSC incorporating FA and WSF.

Data Availability

Data will be provided upon request.

Conflicts of Interest

The authors declare that they have no conflicts of interest.

Acknowledgments

The authors would like to extend their appreciation to the Deanship of Scientific Research at King Khalid University, Saudi Arabia, for funding this work through the Research Group Program under Grant no. RGP. 1/14/42.

References

[1] D.-Y. Oh, T. Noguchi, R. Kitagaki, and W.-J. Park, "CO2 emission reduction by reuse of building material waste in the Japanese cement industry," *Renewable and Sustainable Energy Reviews*, vol. 38, pp. 796–810, 2014.

[2] E. Benhelal, G. Zahedi, E. Shamsaei, and A. Bahadori, "Global strategies and potentials to curb CO2 emissions in cement industry," *Journal of Cleaner Production*, vol. 51, pp. 142–161, 2013.

[3] N. Mahasenan, S. Smith, and K. Humphreys, "The cement industry and global climate changecurrent and potential future cement industry CO_2 emissions," in *Proceedings of the Greenhouse Gas Control Technologies-6th International Conference*, pp. 995–1000, Elsevier, Pergamon, Turkey, 2003.

[4] M. A. Nisbet, M. G. VanGeem, J. Gajda, and M. Marceau, "Environmental life cycle inventory of portland cement concrete," *PCA R&D Serial*, vol. 28, 2000.

[5] R. Kurda, J. de Brito, and J. Silvestre, "Combined economic and mechanical performance optimization of recycled aggregate concrete with high volume of fly ash," *Applied Sciences*, vol. 8, no. 7, p. 1189, 2018.

[6] M. A. Nawaz, L. A. Qureshi, B. Ali, and A. Raza, "Mechanical, durability and economic performance of concrete incorporating fly ash and recycled aggregates," *SN Applied Sciences*, vol. 2, no. 2, p. 162, 2020.

[7] R. Kurad, J. D. Silvestre, J. de Brito, and H. Ahmed, "Effect of incorporation of high volume of recycled concrete aggregates and fly ash on the strength and global warming potential of concrete," *Journal of Cleaner Production*, vol. 166, pp. 485–502, 2017.

[8] Astm-C618, *Standard Specification for Coal Fly Ash and Raw or Calcined Natural Pozzolan for Use in Concrete*ASTM International, West Conshohocken, PA, 2017, http://www.astm.org.

[9] B. Ali, S. S. Raza, R. Kurda, and R. Alyousef, "Synergistic effects of fly ash and hooked steel fibers on strength and durability properties of high strength recycled aggregate concrete," *Resources, Conservation and Recycling*, vol. 168, Article ID 105444, 2021.

[10] R. Kurda, J. D. Silvestre, J. de Brito, and H. Ahmed, "Optimizing recycled concrete containing high volume of fly ash in terms of the embodied energy and chloride ion resistance," *Journal of Cleaner Production*, vol. 194, pp. 735–750, 2018.

[11] R. Kurda, J. de Brito, and J. D. Silvestre, "Combined influence of recycled concrete aggregates and high contents of fly ash on concrete properties," *Construction and Building Materials*, vol. 157, pp. 554–572, 2017.

[12] A. R. Boğa and I. B. Topçu, "Influence of fly ash on corrosion resistance and chloride ion permeability of concrete," *Construction and Building Materials*, vol. 31, pp. 258–264, 2012.

[13] Y. Hefni, Y. A. E. Zaher, and M. A. Wahab, "Influence of activation of fly ash on the mechanical properties of concrete," *Construction and Building Materials*, vol. 172, pp. 728–734, 2018.

[14] B. B. Das and S. P. Pandey, "Influence of fineness of fly ash on the carbonation and electrical conductivity of concrete," *Journal of Materials in Civil Engineering*, vol. 23, no. 9, pp. 1365–1368, 2011.

[15] P. Chindaprasirt, C. Chotithanorm, H. T. Cao, and V. Sirivivatnanon, "Influence of fly ash fineness on the chloride penetration of concrete," *Construction and Building Materials*, vol. 21, no. 2, pp. 356–361, 2007.

[16] D. F. Velandia, C. J. Lynsdale, J. L. Provis, F. Ramirez, and A. C. Gomez, "Evaluation of activated high volume fly ash systems using Na 2 SO 4 , lime and quicklime in mortars with high loss on ignition fly ashes," *Construction and Building Materials*, vol. 128, pp. 248–255, 2016.

[17] S. H. Gebler and P. Klieger, "Effect of fly ash on physical properties of concrete," *Special Publication*, vol. 91, pp. 1–50, 1986.

[18] H. Rolander, *Potential Applications for High-Strength Concrete in Cast In-Situ Structures*, Aalto University, Espoo, Finland, 2019.

[19] M. F. M. Zain, H. B. Mahmud, A. Ilham, and M. Faizal, "Prediction of splitting tensile strength of high-performance concrete," *Cement and Concrete Research*, vol. 32, no. 8, pp. 1251–1258, 2002.

[20] E. Lubloy, "How does concrete strength affect the fire resistance?" *Journal of Structural Fire Engineering*, vol. 11, no. 3, 2020.

[21] V. Afroughsabet, L. Biolzi, and P. J. M. Monteiro, "The effect of steel and polypropylene fibers on the chloride diffusivity and drying shrinkage of high-strength concrete," *Composites Part B: Engineering*, vol. 139, pp. 84–96, 2018.

[22] S. Teng, V. Afroughsabet, and C. P. Ostertag, "Flexural behavior and durability properties of high performance hybrid-fiber-reinforced concrete," *Construction and Building Materials*, vol. 182, pp. 504–515, 2018.

[23] A. B. Kizilkanat, N. Kabay, V. Akyüncü, S. Chowdhury, and A. H. Akça, "Mechanical properties and fracture behavior of basalt and glass fiber reinforced concrete: an experimental study," *Construction and Building Materials*, vol. 100, pp. 218–224, 2015.

[24] A. Akbar and K. M. Liew, "Multicriteria performance evaluation of fiber-reinforced cement composites: an environmental perspective," *Composites Part B: Engineering*, vol. 218, Article ID 108937, 2021.

[25] A. Al-Tikrite and M. N. S. Hadi, "Mechanical properties of reactive powder concrete containing industrial and waste steel fibres at different ratios under compression," *Construction and Building Materials*, vol. 154, pp. 1024–1034, 2017.

[26] M. A. Aiello, F. Leuzzi, G. Centonze, and A. Maffezzoli, "Use of steel fibres recovered from waste tyres as reinforcement in concrete: pull-out behaviour, compressive and flexural strength," *Waste Management*, vol. 29, no. 6, pp. 1960–1970, 2009.

[27] M. Mastali and A. Dalvand, "Use of silica fume and recycled steel fibers in self-compacting concrete (SCC)," *Construction and Building Materials*, vol. 125, pp. 196–209, 2016.

[28] K. M. Liew and A. Akbar, "The recent progress of recycled steel fiber reinforced concrete," *Construction and Building Materials*, vol. 232, Article ID 117232, 2020.

[29] G. Centonze, M. Leone, and M. A. Aiello, "Steel fibers from waste tires as reinforcement in concrete: a mechanical characterization," *Construction and Building Materials*, vol. 36, pp. 46–57, 2012.

[30] C. C. Santos and J. P. C. Rodrigues, "Compressive strength at high temperatures of a concrete made with recycled tire textile and steel fibers," in *Proceedings of the MATEC Web of Conferences*, p. 7004, October 2013.

[31] M. Leone, G. Centonze, D. Colonna, F. Micelli, and M. A. Aiello, "Fiber-reinforced concrete with low content of recycled steel fiber: shear behaviour," *Construction and Building Materials*, vol. 161, pp. 141–155, 2018.

[32] K. Aghaee, M. A. Yazdi, and K. D. Tsavdaridis, "Investigation into the mechanical properties of structural lightweight concrete reinforced with waste steel wires," *Magazine of Concrete Research*, vol. 67, no. 4, pp. 197–205, 2015.

[33] O. Sengul, "Mechanical properties of slurry infiltrated fiber concrete produced with waste steel fibers," *Construction and Building Materials*, vol. 186, pp. 1082–1091, 2018.

[34] G. F. Peng, X. J. Niu, and Q. Q. Long, "Experimental study of strengthening and toughening for recycled steel fiber reinforced ultra-high performance concrete," *Key Engineering Materials, Trans Tech Publ*, vol. 629-630, pp. 104–111, 2015.

[35] A. H. Farhan, A. R. Dawson, and N. H. Thom, "Damage propagation rate and mechanical properties of recycled steel fiber-reinforced and cement-bound granular materials used in pavement structure," *Construction and Building Materials*, vol. 172, pp. 112–124, 2018.

[36] Y. Wang, H. C. Wu, and V. C. Li, "Concrete reinforcement with recycled fibers," *Journal of Materials in Civil Engineering*, vol. 12, no. 4, pp. 314–319, 2000.

[37] M. Ahmadi, S. Farzin, A. Hassani, and M. Motamedi, "Mechanical properties of the concrete containing recycled fibers and aggregates," *Construction and Building Materials*, vol. 144, pp. 392–398, 2017.

[38] M. Nili and V. Afroughsabet, "Combined effect of silica fume and steel fibers on the impact resistance and mechanical properties of concrete," *International Journal of Impact Engineering*, vol. 37, no. 8, pp. 879–886, 2010.

[39] J.-K. Kim, J.-S. Kim, G. J. Ha, and Y. Y. Kim, "Tensile and fiber dispersion performance of ECC (engineered cementitious composites) produced with ground granulated blast furnace slag," *Cement and Concrete Research*, vol. 37, no. 7, pp. 1096–1105, 2007.

[40] Y. Ling, K. Wang, W. Li, G. Shi, and P. Lu, "Effect of slag on the mechanical properties and bond strength of fly ash-based engineered geopolymer composites," *Composites Part B: Engineering*, vol. 164, pp. 747–757, 2019.

[41] Z. Wu, C. Shi, and K. H. Khayat, "Influence of silica fume content on microstructure development and bond to steel fiber in ultra-high strength cement-based materials (UHSC)," *Cement and Concrete Composites*, vol. 71, pp. 97–109, 2016.

[42] İ. B. Topçu and M. Canbaz, "Effect of different fibers on the mechanical properties of concrete containing fly ash," *Construction and Building Materials*, vol. 21, no. 7, pp. 1486–1491, 2007.

[43] V. Afroughsabet, L. Biolzi, and T. Ozbakkaloglu, "Influence of double hooked-end steel fibers and slag on mechanical and durability properties of high performance recycled aggregate concrete," *Composite Structures*, vol. 181, pp. 273–284, 2017.

[44] C. D. Atiş and O. Karahan, "Properties of steel fiber reinforced fly ash concrete," *Construction and Building Materials*, vol. 23, pp. 392–399, 2009.

[45] O. Karahan and C. D. Atiş, "The durability properties of polypropylene fiber reinforced fly ash concrete," *Materials & Design*, vol. 32, no. 2, pp. 1044–1049, 2011.

[46] S. S. Raza, L. A. Qureshi, and B. Ali, "Residual mechanical strength of glass fiber reinforced reactive powder concrete exposed to elevated temperatures," *SN Applied Sciences*, vol. 2, no. 9, 2020.

[47] E. Nazarimofrad, F. U. A. Shaikh, and M. Nili, "Effects of steel fibre and silica fume on impact behaviour of recycled aggregate concrete," *Journal of Sustainable Cement-Based Materials*, vol. 6, no. 1, pp. 54–68, 2017.

[48] M. Papachristoforou, E. K. Anastasiou, and I. Papayianni, "Durability of steel fiber reinforced concrete with coarse steel slag aggregates including performance at elevated temperatures," *Construction and Building Materials*, vol. 262, Article ID 120569, 2020.

[49] Astm-C150, *Standard Specification for Portland Cement*, ASTM International, West Conshohocken, PA, USA, 2018.

[50] Astm-C33, *Standard Specification for Concrete Aggregates*ASTM International, West Conshohocken, PA, USA, 2018.

[51] Astm-C39, *Standard Test Method for Compressive Strength of Cylindrical Concrete Specimens*, ASTM International, West Conshohocken, PA, USA, 2015, http://www.astm.org.

[52] Astm-C469, *Standard Test Method for Static Modulus of Elasticity and Poisson's Ratio of Concrete in Compression,* ASTM International, West Conshohocken, PA, USA, 2014, http://www.astm.org.

[53] Astm-C496, *Standard Test Method for Splitting Tensile Strength of Cylindrical Concrete Specimens*ASTM International, West Conshohocken, PA, 2017, http://www.astm.org.

[54] Astm-C1609, *Standard Test Method for Flexural Performance of Fiber-Reinforced Concrete (Using Beam with Third-Point Loading)*, ASTM International, West Conshohocken, PA, 2019, http://www.astm.org.

[55] Astm-C1202, *Standard Test Method for Electrical Indication of Concrete's Ability to Resist Chloride Ion Penetration*ASTM International, West Conshohocken, PA, 2017, http://www.astm.org.

[56] B. Ali, R. Kurda, B. Herki et al., "Effect of varying steel fiber content on strength and permeability characteristics of high strength concrete with micro silica," *Materials*, vol. 13, no. 24, p. 5739, 2020.

[57] V. Afroughsabet and T. Ozbakkaloglu, "Mechanical and durability properties of high-strength concrete containing steel and polypropylene fibers," *Construction and Building Materials*, vol. 94, pp. 73–82, 2015.

[58] B. Ali, L. A. Qureshi, S. H. A. Shah, S. U. Rehman, I. Hussain, and M. Iqbal, "A step towards durable, ductile and sustainable concrete: simultaneous incorporation of recycled aggregates, glass fiber and fly ash," *Construction and Building Materials*, vol. 251, Article ID 118980, 2020.

[59] A. F. Hashmi, M. Shariq, and A. Baqi, "An investigation into age-dependent strength, elastic modulus and deflection of low calcium fly ash concrete for sustainable construction," *Construction and Building Materials*, vol. 283, Article ID 122772, 2021.

[60] J. Xie, L. Huang, Y. Guo et al., "Experimental study on the compressive and flexural behaviour of recycled aggregate concrete modified with silica fume and fibres," *Construction and Building Materials*, vol. 178, pp. 612–623, 2018.

[61] M. N. Isa, K. Pilakoutas, M. Guadagnini, and H. Angelakopoulos, "Mechanical performance of affordable and eco-efficient ultra-high performance concrete (UHPC) containing recycled tyre steel fibres," *Construction and Building Materials*, vol. 255, Article ID 119272, 2020.

[62] H. U. Ahmed, R. H. Faraj, N. Hilal, A. A. Mohammed, and A. F. H. Sherwani, "Use of recycled fibers in concrete composites: a systematic comprehensive review," *Composites Part B: Engineering*, vol. 215, Article ID 108769, 2021.

[63] O. Onuaguluchi and N. Banthia, "Scrap tire steel fiber as a substitute for commercial steel fiber in cement mortar: engineering properties and cost-benefit analyses," *Resources, Conservation and Recycling*, vol. 134, pp. 248–256, 2018.

[64] M. Khan and M. Ali, "Improvement in concrete behavior with fly ash, silica-fume and coconut fibres," *Construction and Building Materials*, vol. 203, pp. 174–187, 2019.

[65] N. Bouzoubaâ, M. H. Zhang, and V. M. Malhotra, "Mechanical properties and durability of concrete made with high-volume fly ash blended cements using a coarse fly ash," *Cement and Concrete Research*, vol. 31, no. 10, pp. 1393–1402, 2001.

[66] D. B. McDonald, "The rapid chloride permeability test and its correlation to the 90-day chloride ponding test," *PCI Journal*, vol. 39, no. 1, pp. 38–47, 1994.

[67] O. A. Mohamed and W. Al Hawat, "Influence of fly ash and basalt fibers on strength and chloride penetration resistance of self-consolidating concrete," *Materials Science Forum*, vol. 866, pp. 3–8, 2016.

[68] M. Koushkbaghi, M. J. Kazemi, H. Mosavi, and E. Mohseni, "Acid resistance and durability properties of steel fiber-reinforced concrete incorporating rice husk ash and recycled aggregate," *Construction and Building Materials*, vol. 202, pp. 266–275, 2019.

[69] V. Marcos-Meson, G. Fischer, C. Edvardsen, T. L. Skovhus, and A. Michel, "Durability of steel fibre reinforced concrete (SFRC) exposed to acid attack - a literature review," *Construction and Building Materials*, vol. 200, pp. 490–501, 2019.